

## A Compact Dual Sharp Band-Notched UWB Antenna with Open-Ended Slots

Jiabin Xu, Dacheng Dong, Shaojian Chen, Zhouying Liao, and Gui Liu\*

**Abstract**—A compact microstrip-fed antenna with dual band-notched characteristics for ultrawideband (UWB) applications is presented. By introducing two open-ended inverted L-shaped slots, two sharp notches are achieved at frequencies of 3.16–3.70 GHz and 5.10–5.95 GHz for  $VSWR > 2$ . A rectangular slot in the ground plane can improve the impedance bandwidth of the proposed antenna. The prototype occupies a compact area of  $22 \times 26 \text{ mm}^2$ . The measurement results indicate that the proposed antenna can reject the interference with coexisting worldwide interoperability for microwave access (WiMAX) and wireless local area network (WLAN) systems. The proposed antenna shows relatively omnidirectional radiation patterns in the pass band.

### 1. INTRODUCTION

Ultrawideband (UWB) systems have been one of the most prolific wireless communication systems due to the advantages of high data rate, low power consumption, and increased resilience to multipath interference. UWB antennas could be used in several applications such as sensor networks, radar, location tracking, and short range high-data-rate wireless connection. However, the UWB systems operating in 3.1–10.6 GHz frequency band will interference existing wireless communication systems, e.g., worldwide interoperability for microwave access (WiMAX: 3.3–3.6 GHz) and wireless local area network (WLAN) for IEEE 802.11.a (5.15–5.875 GHz). As a critical component of UWB systems, UWB antennas are required to provide dual band-notched frequency response functions to avoid the interference.

Monopole antennas are good candidates for UWB applications due to their attractive merits such as low cost, easy fabrication and low profile. Numerous techniques have been used to design band-notched UWB monopole antennas, such as inserting C-shaped slot [1], etching two split-ring resonator (SRR) slots [2], inserting a half wavelength C-shaped slot [3], inverted-U shaped slot [4], and using inverted V-shaped slot [5]. Other techniques have also been investigated, for instance, using a parasitic inverted-L element [6], etching out two elliptic single complementary split-ring resonators of different dimensions [7], introducing a pair of arc-shaped slots and an open-loop resonator [8], and employing an I-shaped parasitic element [9]. However, most reported band-notched UWB antennas suffer from either single band-notched characteristic [2–6, 9, 10] or larger occupation area [1, 7, 8]. In addition, it is complicated and hard to design UWB antenna with sharp notched bands. Most reported dual band-notched UWB antenna cannot achieve sharp rejection performance at both notched bands [11, 12].

In this paper, a compact dual band-notched antenna is proposed for portable UWB devices. To achieve dual band-notched characteristics, two open-ended inverted L-shaped slots with different dimensions are etched on the radiator. By properly selecting the length and width of both open-ended slots, dual notched bands with sharp skirt can be achieved. Parametric study for the key parameters

---

*Received 22 May 2014, Accepted 19 July 2014, Scheduled 18 August 2014*

\* Corresponding author: Gui Liu (iitgliu2@gmail.com).

The authors are with the College of Physics & Electronic Information Engineering, Wenzhou University, Wenzhou, Zhejiang 325035, China.

is conducted to give a further insight of the antenna characteristics. This design provides the antenna designers more freedom to control both the resonance frequencies and bandwidths of sharp notched bands.

## 2. ANTENNA DESIGN

The geometry of the proposed antenna is illustrated in Figure 1. The proposed antenna consists of a radiating patch which consists of three merged circular discs, and a rectangular slot in the ground plane. The radii of these three circular discs are  $R_1$ ,  $R_2$ , and  $R_3$ , respectively.  $R_1$  equals to  $R_2$ . Two open-ended inverted-L shaped slots with different width and length are used to obtain dual band-notched characteristics. The centre frequencies of both notched-bands can be easily tuned by varying the length of the open-ended slots. Since the configuration of the ground plane has an effect on the characteristics of the antenna, a rectangular slot is etched in the ground plane to improve the impedance bandwidth. The proposed antenna is fabricated on a F4B substrate material with relative dielectric constant of 2.55, thickness of 0.8 mm, and loss tan of 0.003. The proposed antenna structure was numerically investigated and optimized. To further investigate the effect of the key parameters on the performance of the proposed antenna, only one parameter at a time was varied while keeping all the other parameters fixed.

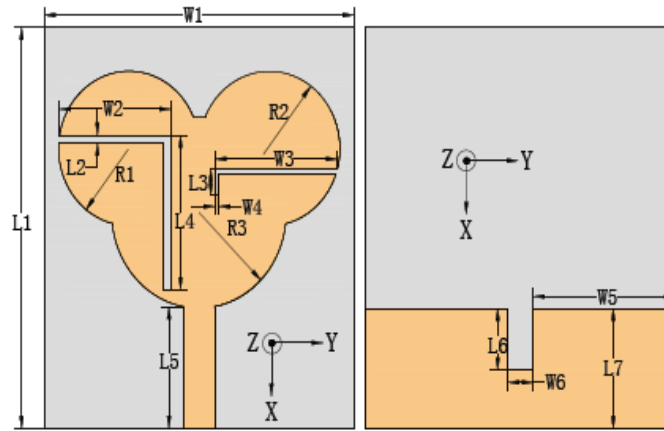


**Figure 1.** Geometry of the proposed antenna. (a) Top view. (b) Bottom view.

### 2.1. Effects of the Slots

Figure 2(a) shows the four structures that were employed to achieve the proposed antenna. Antenna 1 includes the radiating patch and the truncated rectangular ground plane. By etching an inverted L-shaped slot in the radiating patch, a frequency band notch from 3.17 GHz to 4.03 GHz can be observed from the simulated VSWR of antenna 2, as shown in Figure 2(b). The other inverted L-shaped slot is etched on antenna 3 to realize the other notched band from 4.89 GHz to 5.63 GHz. A rectangular slot in the ground plane of the proposed antenna can be employed to improve the impedance matching of antenna 3 and shift the higher notched band to 5.16 GHz to 6.04 GHz, as can be observed from the simulated VSWR of the proposed antenna.

### 2.2. Effects of Various Values of $R_1$ and $R_2$

Figure 3 shows the simulated VSWR of the proposed antenna for various radii  $R_1$  and  $R_2$ . As shown in Figure 3, the resonant frequencies of both notched bands change with  $R_1$  and  $R_2$ . In addition, by properly selecting the radii  $R_1$  and  $R_2$ , impedance bandwidth of the higher notched band can be enhanced.

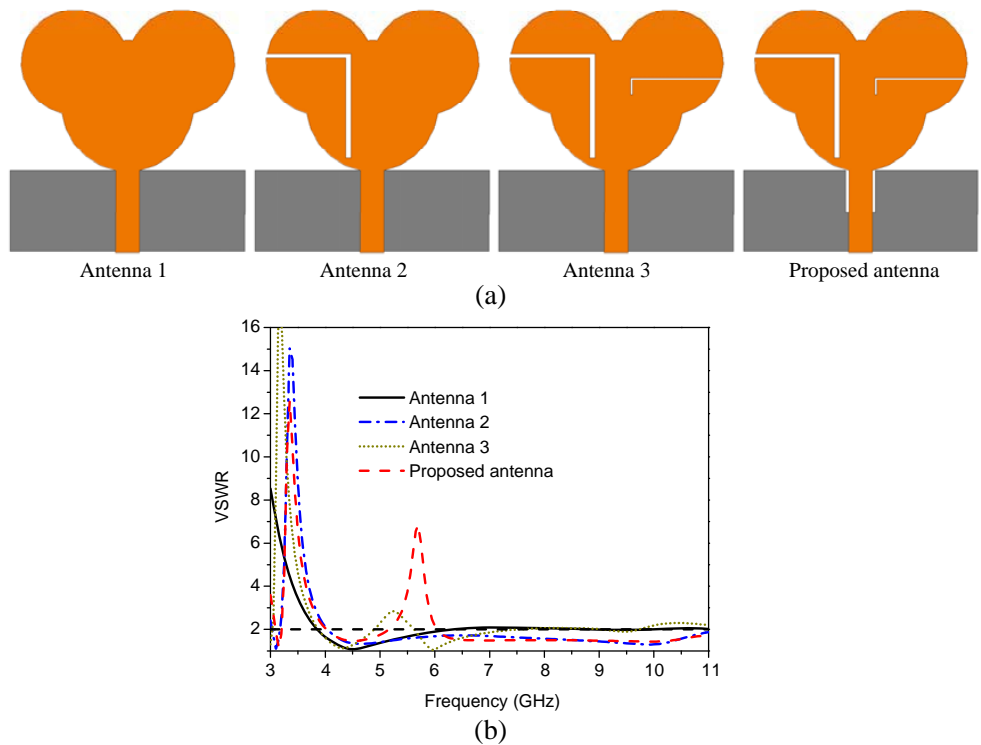


**Figure 2.** Simulated VSWR with different structures.

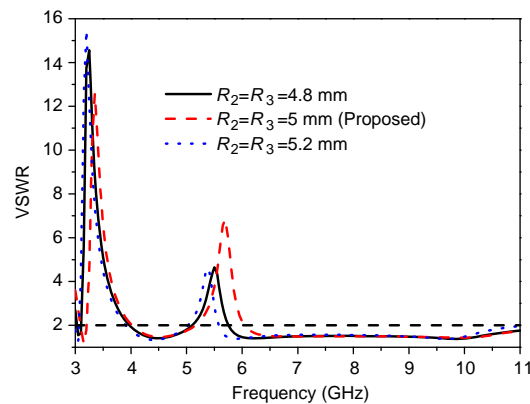


**Figure 3.** Simulated VSWR with different  $R_1$  and  $R_2$ .

### 2.3. Effects of the Length and Width of Both Open-Ended Inverted-L Shaped Slots

In order to investigate the length of the open-ended inverted-L shaped slots on the performance of the proposed antenna, various lengths of both slots have been simulated. We fixed the length of horizontal part of the inverted-L shaped slots and changed the length of the vertical part. Figure 4(a) shows the simulated VSWR for various  $L_4$ , the length of the vertical part of left open-ended inverted-L shaped slot. The total length of left open-ended inverted-L shaped slot is  $7.92 \text{ mm} + L_4$ , which is close to the quarter wavelength of the lower resonance frequency (3.4 GHz). The total length of right open-ended inverted-L shaped slot is  $8.46 \text{ mm} + L_3$ , which is close to the quarter wavelength of the higher resonance frequency (5.5 GHz). As can be observed from Figure 4(b), the total length of right open-ended inverted-L shaped slot mainly affects the resonance frequency of the higher notched-band. Therefore by carefully adjusting the length of both  $L_3$  and  $L_4$ , the resonance frequencies of both notched bands can be tuned.

Figure 5 shows the simulated VSWR for various widths of both open-ended inverted-L shaped slots. It can be seen that adjusting the width of the open-ended inverted-L shaped slot is equivalent to vary the capacitor value, which results in the variation of resonant frequency and bandwidth of notched band. Figure 5(a) shows that the resonant frequency and bandwidth of both notched bands vary with

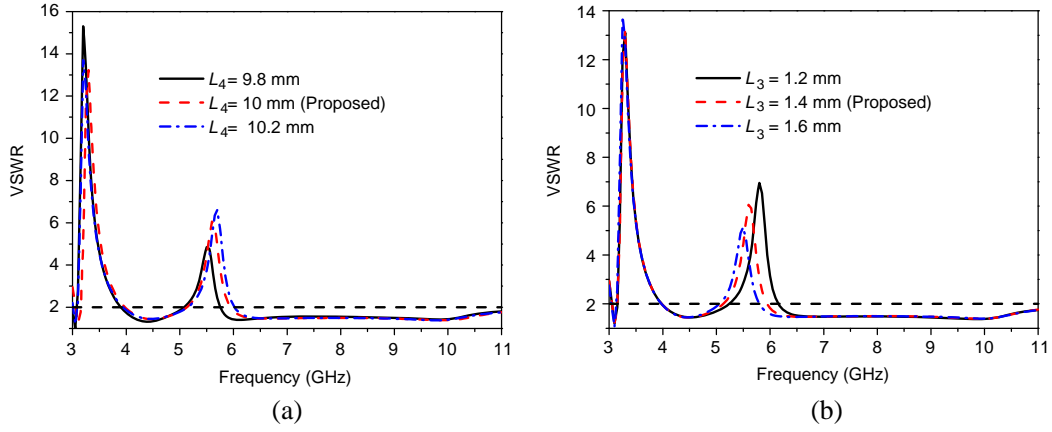


**Figure 4.** Simulated VSWR with different length of open-end slots. (a)  $L_4$ . (b)  $L_3$ .

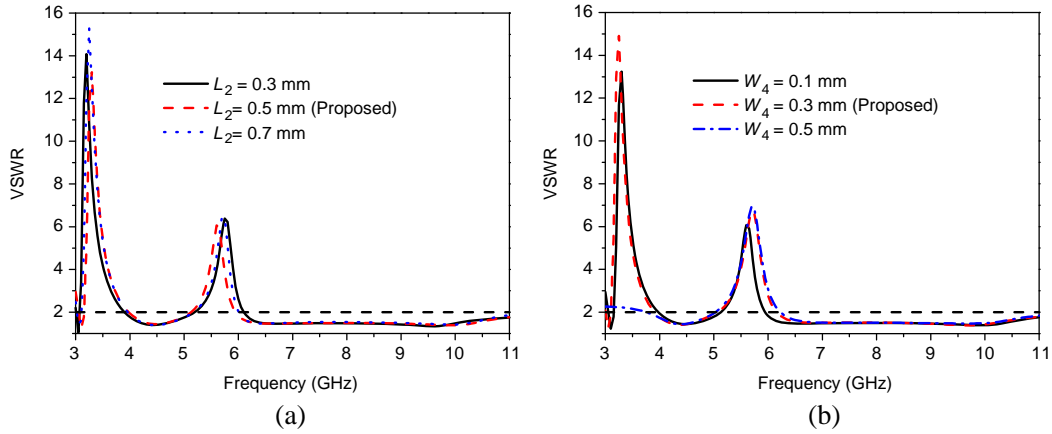


**Figure 5.** Simulated VSWR with different width of open-end slots. (a)  $L_2$ . (b)  $W_4$ .

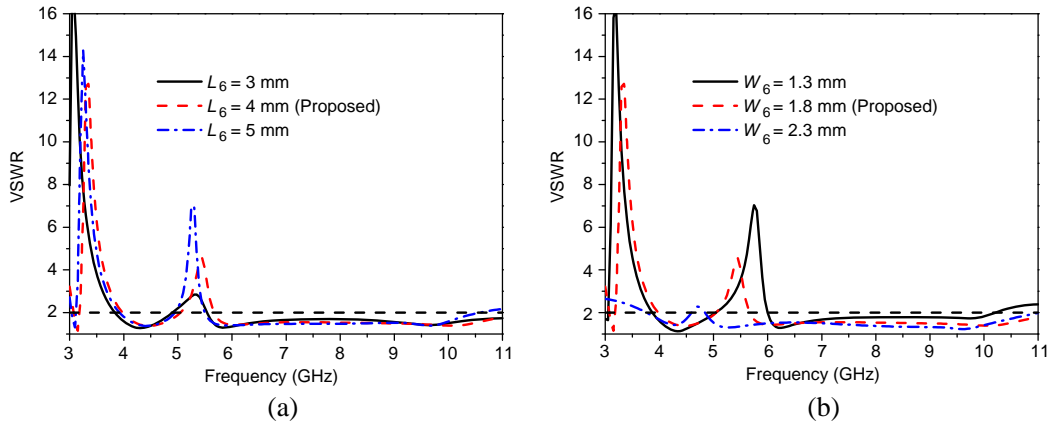


**Figure 6.** Simulated VSWR with different dimensions of the ground plane slots. (a)  $L_6$ . (b)  $W_6$ .

the width of slot. From Figure 5(b), it can be observed that by tuning  $W_4$ , the width of the right open-ended slot, it will be possible to control the resonance frequency and bandwidth of the higher notched-band.

#### 2.4. Effects of the Size of Open-Ended Slot in the Ground Plane

In order to obtain a good impedance matching, a trimmed ground plane was used in the proposed antenna. As shown in Figure 2, the slot in the ground plane can improve the impedance matching. By properly adjusting the size of the notch in the ground plane, good impedance matching over a wide frequency band can be achieved. The optimized dimensions of the slot are  $L_6 = 4$  mm and  $W_6 = 1.8$  mm as shown in Figures 6(a) and (b), respectively.



Figure 7. Photograph of the fabricated antenna. (a) Top view. (b) Bottom view.

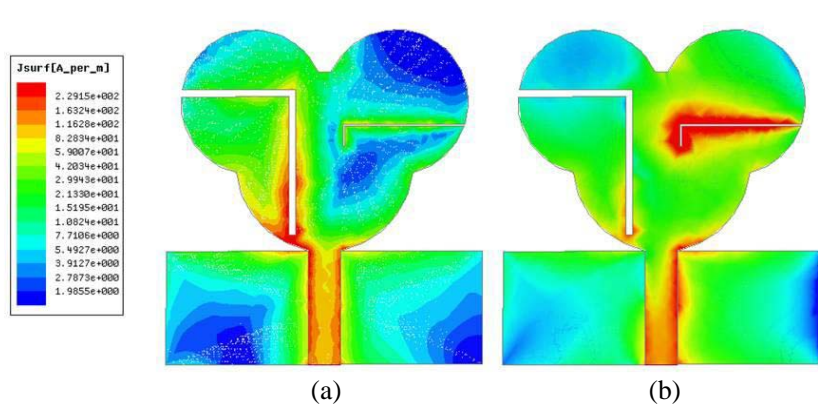


Figure 8. Simulated surface current distributions. (a) 3.4 GHz. (b) 5.5 GHz.

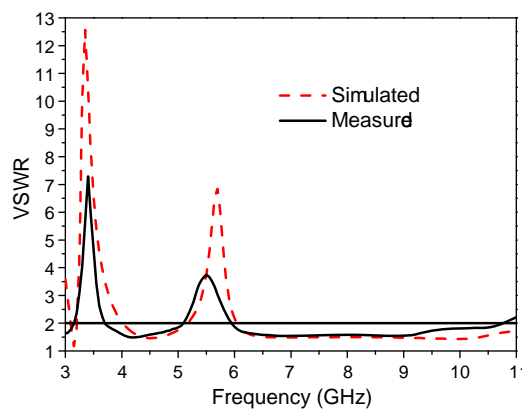
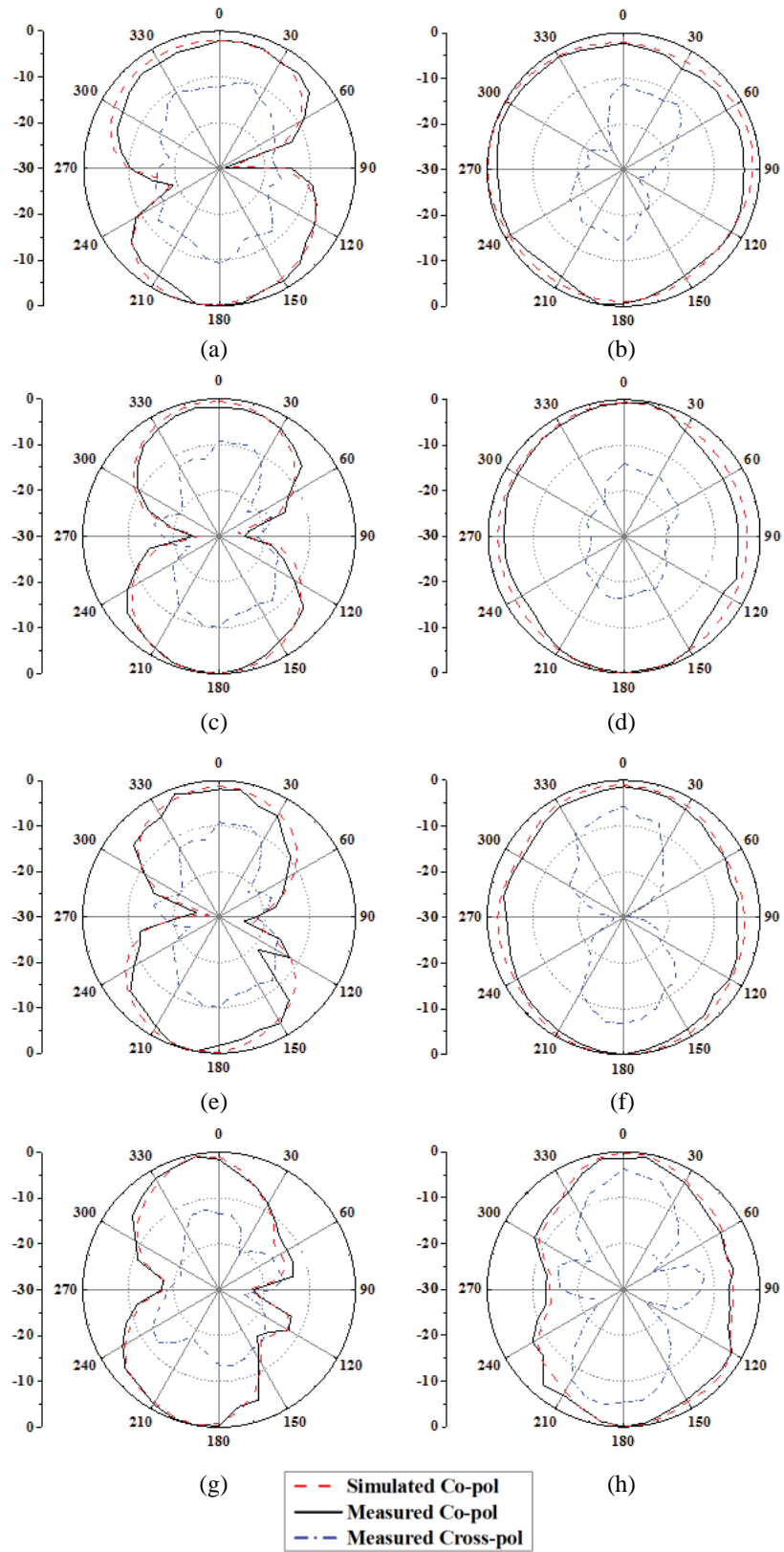
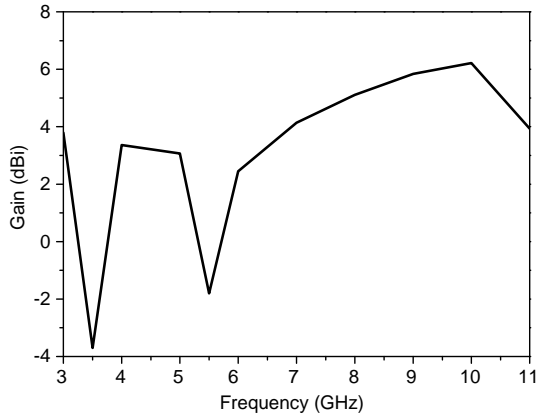


Figure 9. Simulated and measured VSWR of the proposed antenna.



**Figure 10.** Simulated and measured (a), (c), (e), (g)  $E$ - and (b), (d), (f), (h)  $H$ -plane radiation patterns at (a), (b) 3 GHz. (c), (d) 5 GHz. (e), (f) 8 GHz. (g), (h) 10 GHz.



**Figure 11.** Measured peak gain of the fabricated antenna.

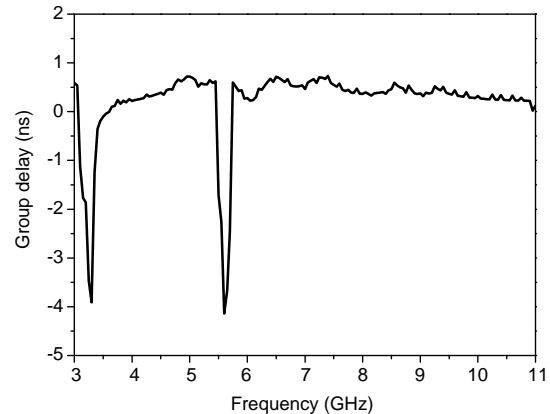


**Figure 12.** Measured group delay.

### 3. SIMULATION AND EXPERIMENTAL RESULTS

The optimal dimensions of the proposed antenna are as follows:  $L_1 = 26$  mm,  $L_2 = 0.5$  mm,  $L_3 = 1.5$  mm,  $L_4 = 9.5$  mm,  $L_5 = 7.9$  mm,  $L_6 = 4$  mm,  $L_7 = 7.8$  mm,  $W_1 = 22$  mm,  $W_2 = 7.92$  mm,  $W_3 = 8.46$  mm,  $W_4 = 0.1$  mm,  $W_5 = 10.1$  mm,  $W_6 = 1.8$  mm,  $R_3 = 6.2$  mm, and  $R_1 = R_2 = 5$  mm. The fabricated prototype of the proposed antenna is shown in Figure 7.

For giving a good physical insight into the operating mechanism of the proposed antenna, Figure 8 shows the current distributions of the proposed antenna at two notched frequencies. As shown in Figure 8(a), at the lower notched frequency (3.4 GHz), the current flows mostly around the edge of the left inverted L-shaped slot. Figure 8(b) presents the surface current distribution at the higher notched frequency (5.5 GHz). It can be observed in Figure 8(b) that the surface current concentrates around the edge of the right inverted L-shaped slot. Therefore, at the notched-bands, the strong capacitive coupling occurs around the edge of the inverted L-shaped slots. The energy is stored around the slots rather than radiated into the air.

Figure 9 shows the simulated and measured VSWR for the proposed antenna. It can be observed that the proposed antenna exhibits ultrawideband performance with dual band-notched functions of 3.16–3.70 GHz and 5.10–5.95 GHz. Both stop bands can avoid interference between UWB systems and WiMAX/WLAN systems. The lower notched band centred at 3.4 GHz is generated by the left inverted L-shaped slot, while the higher notched band centred at 5.5 GHz is achieved by the right inverted L-shaped slot. The slightly discrepancy between simulated and measured results may be caused by the effect of the SMA connector and soldering effects, which have been neglected in the simulation.

Figure 10 shows the measured radiation patterns of the proposed antenna at the selective frequencies of 3, 5, 8, and 10 GHz in  $E$ -plane and  $H$ -plane. It can be observed that the antenna pattern is omnidirectional in the  $H$ -plane ( $yz$ -plane) and dipole-like in the  $E$ -plane ( $xz$ -plane), which is important for wireless communication devices.

The measured peak gain of the proposed antenna is depicted in Figure 11. Since at the notch bands most of the radiated power is reflected back, the gain decreases sharply in the vicinity of 3.5 GHz and 5.5 GHz. Other than the notched bands, the antenna exhibits stable gain performance across the operation band.

The group delay should maintain constant and stable over the entire operating frequency band to avoid undesirable distortion of the radiated and received pulse. Two identical proposed antennas were placed face-to-face with a distance of 100 cm. As shown in Figure 12, the group delay is flat over the entire UWB range except at the notched bands. Therefore the proposed antenna is suitable for transmitting and receiving UWB pulse with little distortion.

#### 4. CONCLUSION

In this paper, a CPW-fed UWB antenna with dual notched-band characteristics has been proposed and fabricated. The dual notched-band operations of the proposed antenna are achieved by using both open-ended inverted L-shaped slots. The proposed antenna exhibits dual notched-band characteristics for both WiMAX (3.3–3.7 GHz) and WLAN (5.15–5.875 GHz) frequency bands. The antenna shows good radiation performance with acceptable gain over the desired frequency bands. The antenna is compact and planar that makes it a good candidate for UWB applications.

#### ACKNOWLEDGMENT

This work was supported in part by the Zhejiang Provincial Natural Science Foundation of China under Grant No. LY12F04002, National Natural Science Foundation of China under Grant No. 61340049, Zhejiang Qianjiang Talents Project under Grant No. QJD1202003, and Technology Foundation for Selected Overseas Chinese Scholar under Grant No. R20130601.

#### REFERENCES

1. Chu, Q.-X. and Y.-Y. Yang, "A compact ultrawideband antenna with 3.4/5.5 GHz dual band-notched characteristics," *IEEE Trans. Antennas Propag.*, Vol. 56, No. 12, 3637–3644, Dec. 2008.
2. Gao, P., S. He, X. Wei, N. Wang, and Y. Zheng, "Compact printed UWB diversity slot antenna with 5.5-GHz band-notched characteristics," *IEEE Antennas Wirel. Propag. Lett.*, Vol. 13, 714–717, Feb. 2014.
3. Chu, Q.-X. and T.-G. Huang, "Compact UWB antenna with sharp band-notched characteristics for lower WLAN band," *Electron. Lett.*, Vol. 47, No. 15, 838–839, Jul. 2011.
4. Seo, Y. S., J. W. Jung, H. J. Lee, and Y. S. Lim, "Design of trapezoid monopole antenna with band-notched performance for UWB," *Electron. Lett.*, Vol. 48, No. 12, 673–674, Jun. 2012.
5. Mohammadi, S., J. Nourinia, C. Ghobadi, and M. Majidzadeh, "Compact CPW-fed rotated square-shaped patch slot antenna with band-notched function for UWB applications," *Electron. Lett.*, Vol. 48, No. 12, 1307–1308, Nov. 2011.
6. Lee, J., K. Kim, H. Ryu, and J. Woo, "A compact ultrawideband MIMO antenna with WLAN band-rejected operation for mobile devices," *IEEE Antennas Wirel. Propag. Lett.*, Vol. 11, 990–993, Aug. 2012.
7. Sarkar, D., K. Sarkar, and K. Saurav, "A compact microstrip-fed triple band-notched UWB monopole antenna," *IEEE Antennas Wirel. Propag. Lett.*, Vol. 13, 396–399, Feb. 2014.
8. Liu, J. J., K. P. Esselle, S. G. Hay, and S. S. Zhong, "Planar ultra-wideband antenna with five notched stop bands," *Electron. Lett.*, Vol. 49, No. 9, 838–839, Jun. 2013.
9. Choi, N., C. Jung, J. Byun, F. Harackiewicz, M. Park, Y. Chung, T. Kim, and B. Lee, "Compact UWB antenna with I-shaped band-notch parasitic element for laptop applications," *IEEE Antennas Wirel. Propag. Lett.*, Vol. 8, 580–582, 2009.
10. Ojaroudi, N., "Application of protruded strip resonators to design an UWB slot antenna with WLAN band-notched characteristic," *Progress In Electromagnetics Research C*, Vol. 47, 111–117, 2014.
11. Akbari, M., M. Khodae, S. Zarbakhsh, and R. Gholam, "A simple UWB antenna with dual stop-band performance using rectangular slot and strip line ended up shorting pin," *Progress In Electromagnetics Research C*, Vol. 42, 83–94, 2013.
12. Nasser, O. and M. Ojaroudi, "Dual band-notched monopole antenna with multi-resonance characteristic for UWB wireless communications," *Progress In Electromagnetics Research C*, Vol. 40, 187–199, 2013.